JAIST Repository
https://dspace.jaist.ac.jp/

Title	Lyotropic ordering for high proton conductivity in sulfonated semialiphatic polyimide thin films
Author(s)	Takakura, Kensaku; Ono, Yutaro; Suetsugu, Kota; Hara, Mitsuo; Nagano, Shusaku; Abe, Takashi; Nagao, Yuki
Citation	Polymer Journal, 51: 31-39
Issue Date	2018-08-03
Type	Journal Article
Text version	author
URL	http://hdl.handle.net/10119/16672
Rights	This is the author-created version of Springer, Kensaku Takakura, Yutaro Ono, Kota Suetsugu, Mitsuo Hara, Shusaku Nagano, Takashi Abe, and Yuki Nagao, Polymer Journal, 51, 2018, 31-39. The original publication is available at www.springerlink.com, https://doi.org/10.1038/s41428-018-0111-1
Description	

JAIST
JAPAN
ADVANCED INSTITUTE OF
SCIENCE AND TECHNOLOGY

Japan Advanced Institute of Science and Technology

Lyotropic Ordering for High Proton Conductivity in Sulfonated Semi-aliphatic Polyimide Thin Films

Kensaku Takakura,[1] Yutaro Ono,[1] Kota Suetsugu,[2] Mitsuo Hara,[2]

Shusaku Nagano,[3] Takashi Abe,[4] and Yuki Nagao[1*]

[1] School of Materials Science, Japan Advanced Institute of Science and Technology, 1-1 Asahidai, Nomi, Ishikawa 923-1292, Japan

[2] Department of Molecular Design & Engineering Graduate School of Engineering, Nagoya University, Furo-cho, Chikusa, Nagoya 464-8603, Japan

[3] Nagoya University Venture Business Laboratory, Nagoya University, Furo-cho, Chikusa, Nagoya 464-8603, Japan

[4] Graduate School of Science and Technology, Niigata University, 8050 Ikarashi 2-no-cho, Nishi-ku, Niigata 950-2181, Japan

Corresponding Author

*(Y.N.) E-mail: ynagao@jaist.ac.jp. Telephone: +81(Japan)-761-51-1541. Fax: ;81(Japan)-761-51-1149.

Running Head

Proton Conduction in Oriented Sulfonated Polyimide Films

Abstract

Influence of the semi-aliphatic backbone on the molecular ordering and proton conductivity was investigated compared to the rigid aromatic backbone in highly proton-conductive organized polyimide thin films. We newly synthesized two alkyl sulfonated semi-aliphatic polyimides (ASSPIs) with different molecular weights and investigated their molecular organized structure, proton conductivity, water uptake, and dissociation state of protons from sulfonic acid groups in thin films by *in-situ* measurements for grazing incidence small-angle X-ray scattering (GISAXS), quartz crystal microbalance (QCM), Fourier transform infrared (FT-IR) spectra, and impedance spectra. Declining of planarity in the semi-aliphatic backbone reduced the aggregative character and molecular ordering in the lyotropic liquid crystalline (LC) structure. However, the higher molecular weight ASSPI exhibited the oriented lamellar structure in spite of lower planarity of the main chain. The proton conductivity of the oriented lamellar thin film displayed a more than half order of magnitude higher value of 1.5×10^{-1} S cm^{-1} than that of the non-oriented lamellar thin film (3.0×10^{-2} S cm^{-1}) at 25°C and 95% RH. These results indicate that, in sulfonated polyimide thin films, the lamellar orientation greatly contributes to the high proton conductivity in the ASSPI thin films.

Keywords : Sulfonated polyimide, Thin film, Molecular orientation, Organized structure, Proton conductivity, Lyotropic liquid crystalline property

Introduction

Structural control of highly ion-conductive channels is a notable strategy for energy conversion system, water treatment, and biotechnology [1-5]. Nanostructured liquid crystals that self-organize into dimensionally ordered states represents a promising approach to the development of structural control of ion-conductive materials [6, 7]. Thermotropic and lyotropic liquid crystal properties can drive organized structure of various kinds. Kato *et al.* demonstrated switchable ionic conductivities induced by a rectangular-hexagonal phase transition in wedge-shaped liquid-crystalline (LC) ammonium salts [8]. Several groups have also reported relations between ionic conductivity and LC structure with thermotropic and lyotropic liquid crystal properties [9-12].

Designing phase-separated conductive channels composed of hydrophobic backbones and hydrophilic parts is a fundamentally important strategy to create highly proton-conductive materials [13-16]. Typical proton exchange membranes (PEMs) have sulfonic acid groups attached to the hydrophobic polymer as a side chain [17]. State-of-the-art membranes are based on perfluorosulfonic acid (PFSA) ionomers such as Nafion [13, 18, 19]. They exhibit high levels of proton conductivity, water transport, and durability. Protons are transported through water-swollen conductive channels. Understanding the relation between the structure and proton transport property is fundamentally important, but such attempts have often been

hampered in many highly proton-conductive polymers because less structural information can be derived from an amorphous or amorphous-like nature.

Our recent studies have elucidated that proton conductivity enhancement originates from the improvement of molecular ordering and main chain orientation of LC domains in alkyl sulfonated polyimide (ASPI) thin films [20-23]. Actually, ASPI thin films with rigid backbones exhibit lamellar organized structure by water uptake using a lyotropic LC property. However, no report describes the influence of the semi-aliphatic backbones on the organized structure and proton conductivity of alkyl-sulfonated polyimide thin films.

This study elucidated the relation between organized structure and proton conductivity by introduction of a semi-aliphatic structure in the main chain. Lower planarity of backbones can change the organized molecular structure and ordering in the lyotropic LC structure. For polyimides without sulfonic acid groups, Ando *et al.* reported the intermolecular aggregation structures in thin films of fully aromatic polyimides and semialiphatic polyimides by grazing incidence X-ray scattering measurement [24]. In our work, the lyotropic LC structure and proton conductivity were assessed in two alkyl sulfonated semi-aliphatic polyimide (ASSPI) films with different molecular weights by *in-situ* studies of grazing incidence small-angle X-ray scattering (GISAXS), quartz crystal microbalance (QCM), Fourier transform infrared spectra (FT-IR) and impedance analyses. From those results, we conducted systematic

evaluations of the molecular structure, proton conductivity, water uptake, and dissociation state of protons from sulfonic acid groups in thin films. Two ASSPI thin films exhibited different orientation of lamellar structure and proton conductivity. On the other hand, water uptake isotherms and the proton dissociation properties from sulfonic acid groups are almost identical in the two thin films. Therefore, the orientation of the lyotropic lamellar structure largely contributes to the proton conductivity enhancement. Our results indicate that not only main chain planarity but also the increment of molecular weight affects the lyotropic LC structure and moreover the oriented lamellar structure enhanced proton conductivity.

Materials & Methods

Materials

3,3'-Dihydroxybenzidine, 1,3-propanesultone, 9,10-dihydro-9-oxa-10-phosphaphenanthrene 10-oxide (DOPO) and 1,2,4,5-cyclohexanetetracarboxylic dianhydride (HPMDA) were purchased from Tokyo Chemical Industry Co. Ltd., Japan and were used without further purification. 3,3’-Bis(sulfopropoxy)-4,4’-diaminobiphenyl (3,3’-BSPA) was synthesized from 3,3’-dihydroxybendizine and 1,3-propanesultone as described in the literature [22]. Acetone and m-cresol were purchased from Wako Pure Chemical Ind. Ltd., Japan. Triethylamine (TEA) was used as received from Kanto Chemical Co. Inc., Japan.

Synthesis of ASSPI

The ASSPIs of different molecular weights were synthesized using a similar polymerization scheme. Scheme 1 represents the synthesis of the higher molecular weight (HM_w) ASSPI. For HM_w ASSPI, DOPO was used as the catalyst, whereas that was not used in lower molecular weight (LM_w) ASSPI case. Polymerization was conducted using 3,3'-BSPA (0.46 g), HPMDA (0.22 g), DOPO (0.86 g), m-cresol (5 ml), and TEA (0.3 ml) in a 50 mL three-necked round-bottomed flask with a mechanical stirrer under an argon atmosphere. m-Cresol was used as the solvent. After reaction for 25 h at 180°C, the polymerized mixture was poured dropwise into cooled acetone and was washed by centrifugation. The final product was dried under vacuum and was subjected again to an ion-exchange process using Amberlyst. According to the previous literature [25], molecular weight and polydispersity were examined by a gel permeation chromatography (GPC) and results are shown in Table S1. In this scheme, we obtained the ASSPI polymer with high molecular weight (HM_w, 4.0×10^4). We also obtained the ASSPI polymer with lower molecular weight (LM_w, 2.5×10^4), which was polymerized according to the same scheme without DOPO (Scheme S1). Obtained product was characterized ^{1}H NMR and FT-IR spectra (Figure S2 and S3). We selected it as comparison. (Figure S4 shows GPC results.) The degree of sulfonation for the final product was estimated from ^{1}H NMR data as more than 98%. The calculated ion exchange capacity (IEC) was 2.9 meq. g^{-1}.

Scheme 1. Synthesis of higher molecular weight alkyl sulfonated semi-aliphatic polyimide.

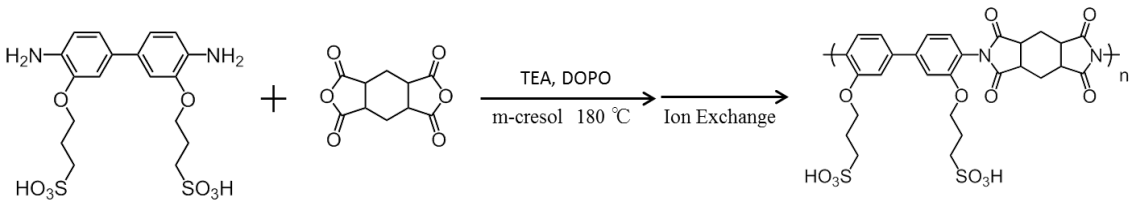

Preparation of Thin Films

ASSPI thin films onto Si, SiO_2 substrates and SiO_2-coated 9 MHz quartz crystals (Seiko EG&G Co. Ltd.) were prepared from 5 wt% of ASSPI solution with a mixed solvent of Milli-Q water and THF by a spincast method with a spin-coater (ACT−200D; Active Co. Ltd.). Before film deposition, the substrates were washed by soaking in 2-propanol and plasma treatment with a vacuum plasma system (Cute-MP; Femto Science, Korea) to improve surface hydrophilicity. Thicknesses of the thin films were measured using a white interference microscope (BW-S506; Nikon Corp.) and an atomic force microscope (AFM, VN-8000; Keyence Co.).

Grazing Incidence Small-angle X-ray Scattering (GISAXS)

GISAXS measurements were taken with a FR-E X-ray diffractometer equipped with R-AXIS IV two-dimensional (2D) detector (FR-E; Rigaku Corp.). Thin film samples were placed into a humidity-controlled cell with X-ray transparent polyester film (Lumirror) windows. To control the humidity, nitrogen carrier gas was used as received from the gas cylinder without further dehumidification . Voltage of 45 kV, current of 45 mA, and irradiation time of 1 h were applied to create copper Cu Kα radiation (λ = 0.1542 nm) with beam size of approximately 300 μm × 300 μm. The camera length was 300 mm. X-ray scattering patterns were recorded on an imaging plate (Fujifilm Corp.). The incident angle was chosen as 0.20° – 0.22°. For 1-D out-of-plane and in-plane patterns, the integrated regions were taken, respectively, between -0.5° to +0.5° as 2 θ from the center (0°) and the width of 1° as 2θ, respectively.

Thin-Film Conductivity Measurements

For conductivity measurements of ASSPI thin films, impedance spectroscopy measurements were taken using a two-probe method to obtain proton conductivity parallel to the film surface with frequency response analyzer and high-frequency dielectric interface (SI1260 and SI1296; Solartron Analytical). Gold paste was used as the thin film electrodes for the conductivity measurements. The relative humidity (RH) and temperature were monitored by a computer-controlled environmental test chamber (SH-221; Espec Corp.). Impedance data were collected

by application of an alternating potential of 50 mV over a frequencies ranging from 10 MHz to 1 Hz. The thin-film conductivity (σ) was calculated from the resistance value (*R*) obtained directly from the impedance measurements using

$$\sigma = \frac{d}{Rlt}, \quad (1)$$

where *d* represents the space between the gold electrodes, t stands for the film thickness, and *l* expresses the contact electrode length.

Water Uptake Measurements of Thin Films

Water uptake of ASSPI thin films was measured by an *in-situ* QCM system. The relative humidity (RH) was controlled by a dry N_2 gas and humidified streams using humidity controller (BEL Flow; BEL Japan Inc.). QCM substrates were connected to an oscillation circuit with a DC power supply and frequency counter (53131A; Agilent Technologies Japan Ltd.). The QCM substrate was placed in an in-house constructed humidity chamber with a high-resolution RH sensor. The frequencies found before and after spin-coating of the QCM substrate were confirmed at the dry N_2 stream for determined the mass of dry film by the Sauerbrey equation as

$$\Delta m = \frac{S \times \sqrt{\rho \mu}}{2 \times F^2} \times (-\Delta F), \quad (2)$$

where S denotes the electrode surface area, ρ stands for the quartz density, μ expresses the shear modulus of quartz, and F signifies the fundamental frequency of the QCM substrate. Water content λ, the number of water molecules per sulfonic acid, was calculated as shown below,

$$\lambda = (\frac{m}{m_0} - 1) \times \frac{EW}{M_{H_2O}}, \quad (3)$$

In that equation, m represents the film mass at each RH, m_0 stands for the film mass of at the 0% RH, M_{H_2O} is the molecular mass of water molecular, and EW expresses the equivalent of each ASSPI.

***In-situ* FT-IR**

The dissociation state of protons from sulfonic acid groups was examined by *in-situ* FT-IR measurements. ASSPI thin films on Si wafers were set in homemade cell. CaF_2 windows were used for the humidity-controlled cell. Then transmission *in-situ* FT-IR measurements were taken using an FT-IR spectrometer (Nicolet 6700; Thermo Fisher Scientific Inc.) equipped with deuterium triglycine sulfate (DTGS) detector. The relative humidity (RH) was controlled by a humidity generator (me-40DP-2PW; Micro equipment). Thicknesses of films prepared on oxidized Si substrates used for this measurement were approximately 500 nm.

Results and discussion

***In-situ* GISAXS**

GISAXS is powerful tool for reveal molecular packings and molecular orderings in molecular organized thin films [26-28]. Matsui *et al.* showed anisotropic proton conductivity in a polymer multilayer thin film with a well-defined lamellar structure confirmed from GISAXS measurements [29]. Proton conductivity was enhanced by the formation of 2D hydrogen-bonding networks in multilayer nanosheets [30, 31]. To investigate the influence of the semi-aliphatic main chain on the lyotropic organized structure, RH-dependent *in-situ* GISAXS measurements were conducted in the ASSPI thin films. 2D scattering images are shown in Figures 1 a–d and Figures 2 a–d for HM_w and LM_w ASSPI thin films, respectively. Series of in-plane and out-of-plane 1D profiles for HM_w and LM_w thin films with various RH are depicted in Figures 1e, f and Figures 2e, f, respectively. In the in-situ GISAXS measurements of the HM_w thin film, scattering peaks in the out-of-plane position were observed around small angle region of 2θ = 4–5° (d = 2.1–2.7 nm) at more than 70% RH (Figures 1c and 1d). The out-of-plane peaks in the HM_w thin film implied that the repeating ordered structure was formed perpendicularly to the substrate plane in the thin film. Our earlier work demonstrated that the out-of-plane scatterings were attributed to the lamellar structure in the in-plane stacked hydrophobic polyimide backbone with hydrophilic sulfonated side chains [21]. In a high RH condition, this out-of-plane scattering peak was enhanced and shifted to the smaller angle region

(Figure 1f). At 95% RH, the out-of-plane peak reached 3° (d = 2.7 nm); it was markedly enhanced relative to X-ray specular peak. These results reflect that the lamellar structure is constructed by containing water through the thin film, which is incorporated selectively into the interlamellar space. The scattering peak shift and intensity enhancement with humidity respectively represented the lamellar expansion and ordering of the amphiphilic lamellar structure to the out-of-plane direction. Molecular ordering is enhanced as the lamellar spacing expands to the out-of-plane direction as humidity increases further. On the other hand, the LM_w thin film exhibited semicircle scattering at high humidity condition more than 70% RH (Figure 2d-f) unlike the anisotropic scattering in the HM_w thin film. In the in-plane profile, the scattering shifted to the small angle region as humidity (Figure 2e), which indicate the formation of the same lamellar structure as the HM_w thin film. In the out-of-plane direction, however, peak shifts were not clearly observed due to weak scattering intensity. The semicircle scattering suggests the isotropic structure, therefore the LM_w thin film formed a non-oriented lamellar structure.

Ando and co-workers have discussed details of main chain aggregations by ch-pack as an intermolecular main chain packing and π-stack as an aromatic ring stacking in both aromatic and semialiphatic polyimides with no sulfonated alkyl side chains [24]. These polyimides consisting of diaminocyclohexylmethane and pyromellitic dianhydride form smectic LC-like ordered structure by the main chain aggregations. Alkyl sulfonated aromatic polyimides exhibit

the scatterings attributed to the periodic monomer unit length and ch-pack for the polyimide main chain in the in-plane and out-of-plane positions, respectively [20-23, 25]. The scatterings imply the smectic LC ordering of the intermolecular aggregation in the lyotropic lamellar structure. However, in the present both cases of ASSPI thin films, the scatterings due to the main chain aggregations were not observed. Probably, the non-planar aliphatic rings in the ASSPI thin films inhibit the intermolecular aggregation of the main chain in the lyotropic lamellar structure, so that the main chain smectic ordering is not formed. Thereby, ASSPI thin films only exhibit the scattering due to the lyotropic lamellar structure at high humidity conditions compared to the aromatic polyimide thin films. On the other hand, the HM_w thin film forms the oriented lamellar structure, although the LM_w thin film exhibits the non-oriented one. The reason for the structural difference might derive from the amount of shorter main chains in ASSPI (Figure S4). Polarized optical microscope observation clearly revealed the difference of the long range ordering and LC domain size between the HM_w and LM_w thick films (Figure S5). A birefringence textures were obviously observed in the HM_w film (Figure S5a, b), whereas LM_w film only exhibited an image close to the dark field (Figure S5c, d). These clearly indicate that the LM_w film has less long range order and small domain size. Hereinafter, we respectively designate HM_w thin film as an Oriented lamellar thin film and LM_w thin film as a Non-oriented lamellar thin film.

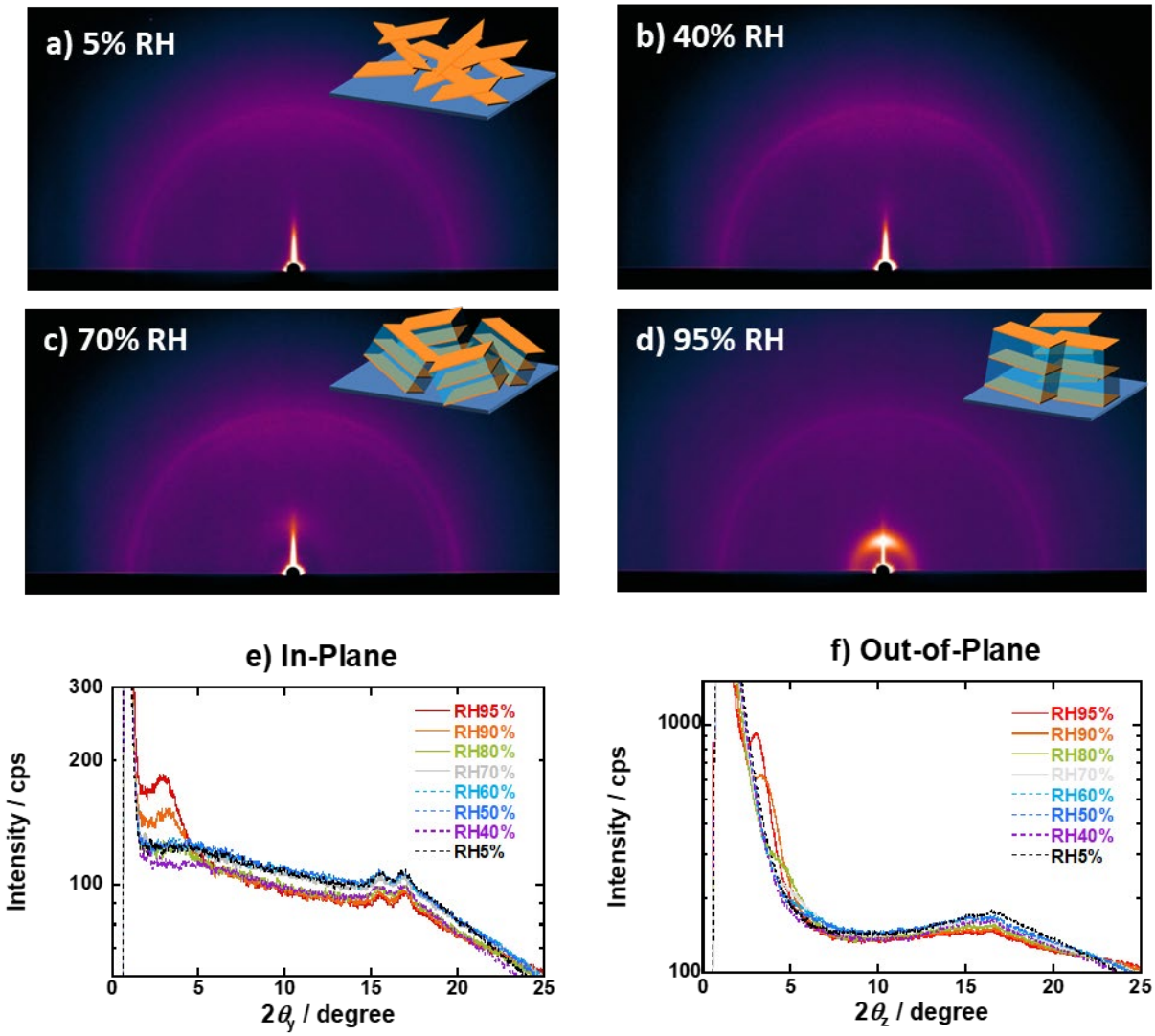

Figure 1. GISAXS results for the HM_w film. Panels a, b, c, and d respectively show the 2D GISAXS patterns at 5% RH, 40% RH, 70% RH, and 95% RH. The humidity-dependent 1D GISAXS profiles in the (e) in-plane and (f) out-of-plane directions of the Oriented lamellar thin film are also shown. The scattering arcs at the positions of 16 and 17 deg result from diffraction of Lumirror films used as the windows for humidity-controlled GISAXS cells.

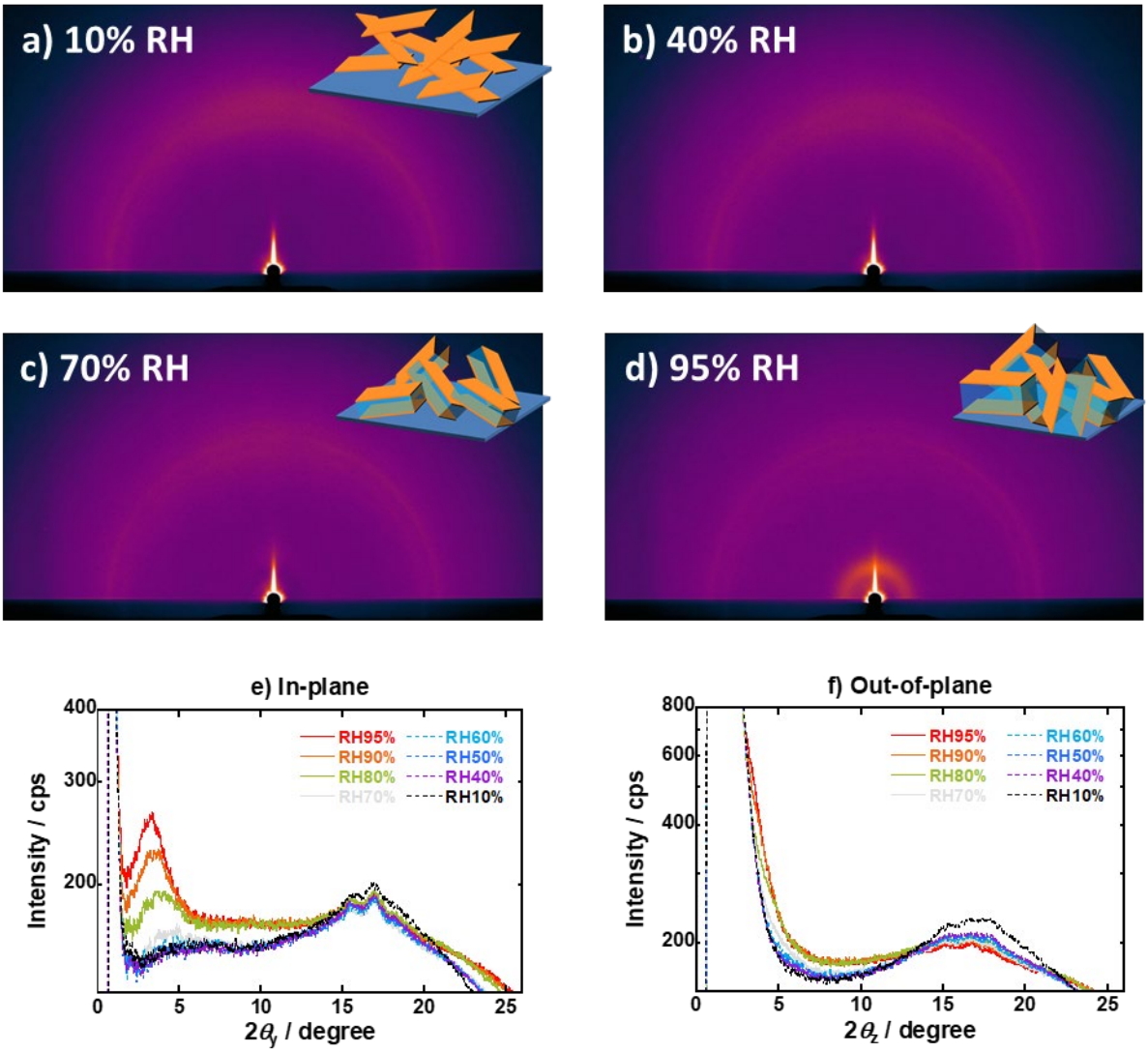

Figure 2. GISAXS results for the LM_w film. Panels a, b, c, and d respectively depict 2D GISAXS patterns at 10% RH, 40% RH, 70% RH, and 95% RH. The humidity-dependent 1D GISAXS profiles in the (e) in-plane and (f) out-of-plane directions of the Non-oriented lamellar thin film are also shown. The scattering arcs at positions of 16 and 17 deg result from diffraction of the Lumirror film used as windows for the humidity-controlled GISAXS cell.

Proton Conductivity

Figure 3 depicts RH-dependent proton conductivity plots for both the Oriented lamellar and Non-oriented lamellar thin films. A linear increase in conductivity was observed by the increase in RH, which is similar for both the Oriented lamellar and Non-oriented lamellar thin films. However, the proton conductivity of the Oriented lamellar film displayed a more than half order of magnitude higher value of 1.5×10^{-1} S cm^{-1} (at 25°C and 95% RH) than that of the Non-oriented lamellar thin film (3.0×10^{-2} S cm^{-1} at 25°C and 95% RH). At the high RH region, this higher proton conductivity is probably obtained by improved molecular ordering and oriented lamellar structure arising from increased molecular weight. Generally, the IEC value is responsible for proton conductivity under high RH conditions [32, 33]. In present work, however, the IEC value is fixed because of the same chemical structure of ASSPI. From the lamellar structure observed in the GISAXS measurement, the hydrophilic sulfonic acid side chains and hydrophobic polyimide main chains are segregated to form the lamella structure parallel to the substrate. In the high humidity condition, the hydrophilic sulfonic layers are selectively hydrated and expanded upon the adsorption of water molecules. Such continuously formed hydrophilic layers in the highly ordered structure promote the marked enhancement of conductivity. To elucidate whether this increment of proton conductivity derives from structural effects or water uptake, *in-situ* QCM measurements were conducted.

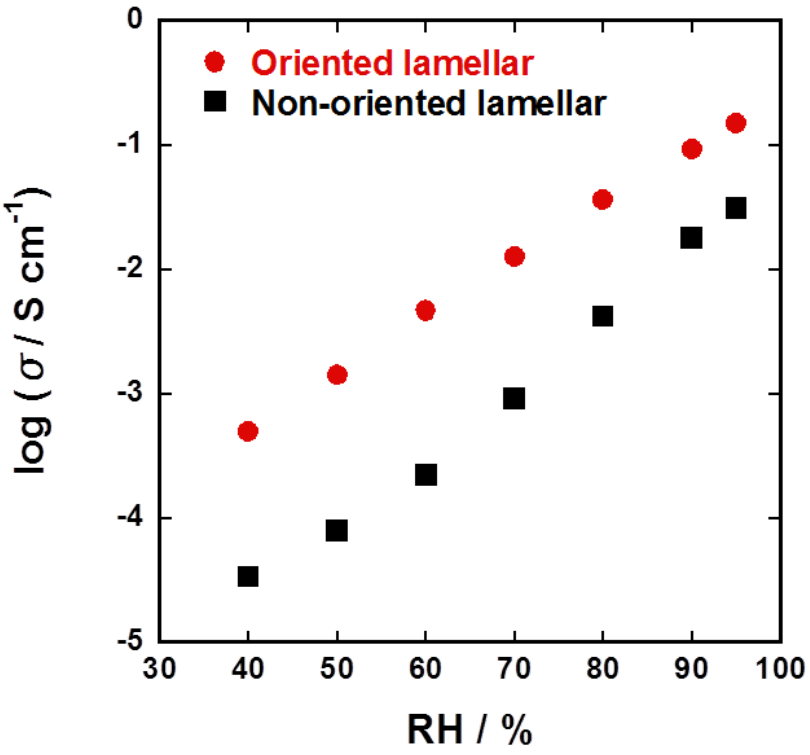

Figure 3. RH-dependent proton conductivity plots for both the Oriented lamellar and Non-oriented lamellar thin films at 298 K.

Water Uptake

Water uptake for the proton exchange membrane affects proton conductivity because water facilitates the transport of protons through the membrane [34]. Figure 4 shows RH-dependent water uptake plots for both the Oriented lamellar and Non-oriented lamellar thin films. The water uptake for both the films increased concomitantly with increasing RH, reaching a value of $\lambda = 16$ in the Oriented lamellar thin film and $\lambda = 14$ in the Non-oriented film. Although no difference was found in the water uptake at low humidity (30–80% RH), the Oriented lamellar

thin film absorbs a little more water molecules than the Non-oriented film. The slightly higher water uptake in the Oriented film results from the anisotropic expansion normal to the substrate plane at high RH condition as observed in GISAXS results.

To elucidate the relation between conductivity and water uptake, plots of conductivity vs. λ were shown in Figure 5. When the proton conductivity is compared at the same λ value, the Oriented lamellar thin film showed more than a half order of magnitude higher proton conductivity than the Non-oriented films. This fact clearly interprets that the water adsorption is not responsibility of the enhancement of proton conductivity. Hence, we inferred that the oriented lamellar structure facilitates proton conductivity and engenders higher proton conductivity at the high RH region.

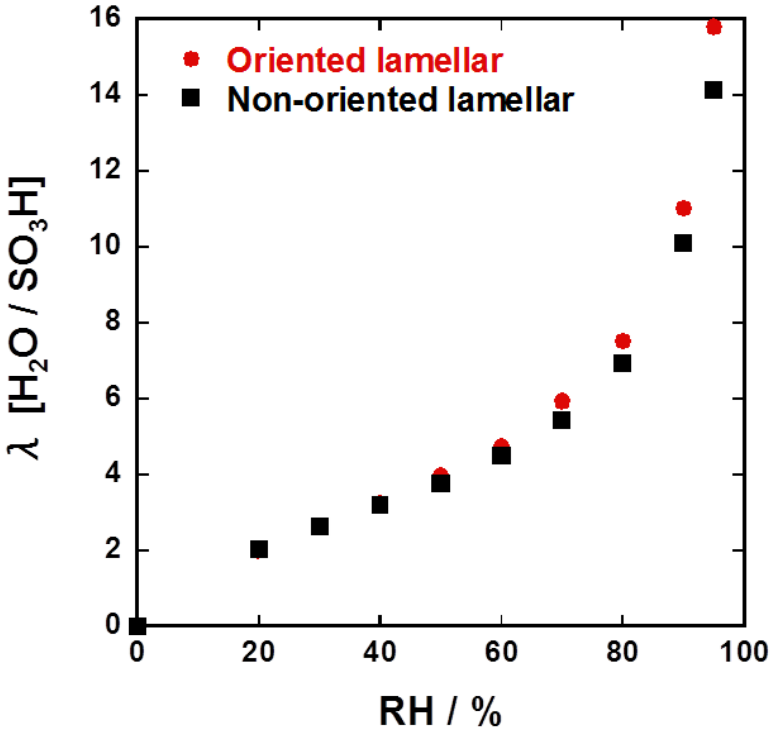

Figure 4. RH-dependent water uptake plots for both the Oriented lamellar and Non-oriented lamellar thin films.

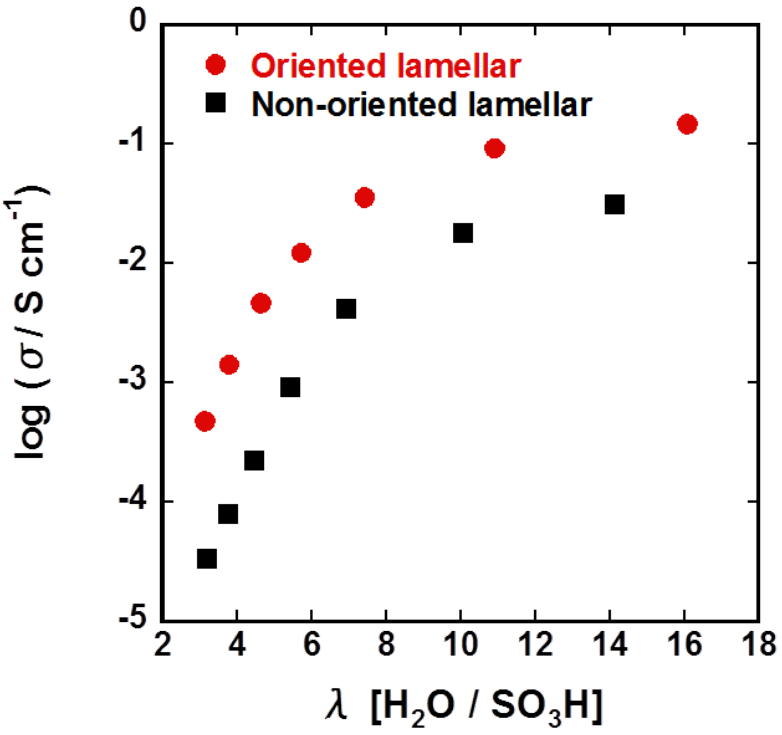

Figure 5. Proton conductivity plots for both the Oriented lamellar and Non-oriented lamellar thin films as a function of the λ value.

Dissociation State of Protons from Sulfonic Acid Groups using *In-situ* FT-IR.

To evaluate dissociation of proton at sulfonic acid groups in the conductivity change, *in-situ* FT-IR measurements under controlled humidity were conducted. Figure 6 shows humidity-dependent FT-IR spectra for the Oriented lamellar and Non-oriented lamellar thin films. The peaks were clearly observed at the bands of 1715, 1640, 1200, and 1030 cm^{-1} corresponding to the ν_{as}(C=O) symmetric stretching vibrations of imide groups, δ(H-O-H), $\nu_{as}(SO_3^-)$ and $\nu_s(SO_3^-)$, respectively. With humidity increase, the absorbance of these peaks was enhanced. The amount

of dissociated protons could be estimated by the absorbance due to the $\nu_s(SO_3^-)$ band. Figure 7 depicts the absorbance of the $\nu_s(SO_3^-)$ band at 1030 cm^{-1} portrayed as a function of the λ value. The absorbance of the $\nu_s(SO_3^-)$ bands increased with the λ value and was saturated for $\lambda > 6$ in both the Oriented lamellar and Non-oriented lamellar thin films. The saturation of the $\nu_s(SO_3^-)$ band absorbance suggests that dissociation of proton at sulfonic acid groups almost completed in relatively low water uptake around $\lambda = 6$. However, the proton conductivity increases considerably over $\lambda = 6$ from Figure 5. Miyatake *et al.* reported a similar tendency to correlate the proton dissociation of sulfonic acid groups and proton conductivity during hydration process in a sulfonated block poly(arylene ether sulfone ketone) membrane [33, 35]. Besides, the both Oriented and Non-oriented films exhibited essentially the same behaviors. Therefore, the dissociation state of proton at sulfonic acid groups is also not responsible for the enhancement of proton conductivity in the Oriented lamellar thin film.

In our earlier work, the highly proton-conductive organized structure was obtained using the lyotropic LC property derived from rigid aromatic main chains. In present work, the influence of the semi-aliphatic structure was discussed. The molecular ordering weakens as a result of the lessened planarity of the main chain because of suppressed the (π-stack) aggregation of the main chain in the lyotropic lamellar structure. The degree of molecular ordering is found to be improved with increasing molecular weight. An oriented lamellar organized structure is

obtained. Although the IEC values, the water uptake and dissociation behavior of proton are identical in both films, the Oriented lamellar film exhibits a half order of magnitude higher proton conductivity compared to the Non-oriented film. Therefore, we inferred that the oriented lamellar structure enhanced proton conductivity more than the non-oriented lamellar structure did.

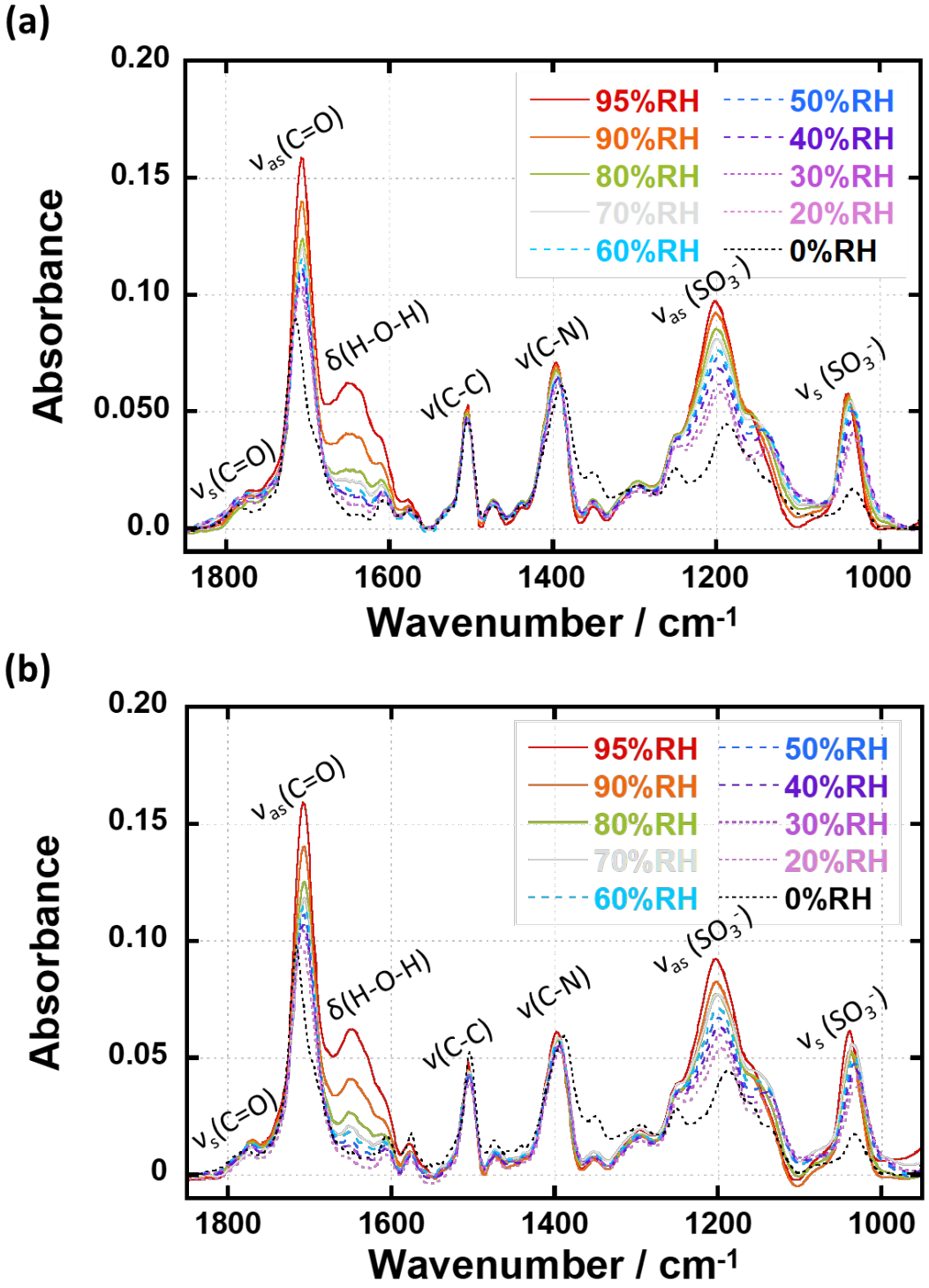

Figure 6. Humidity-dependent FT-IR spectra of (a) Oriented lamellar thin film and (b) Non-oriented lamellar thin film.

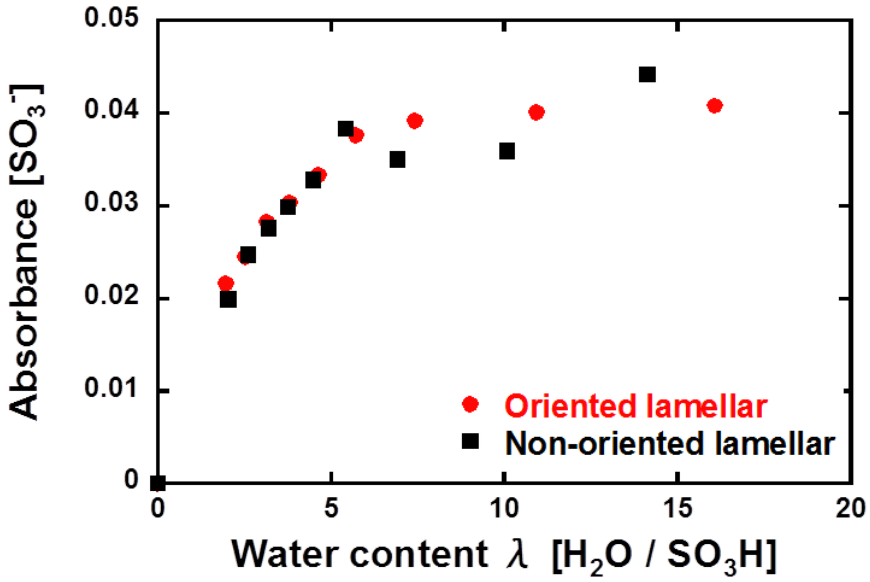

Figure 7. Change of the absorbance of $\nu_s(SO_3^-)$ of the ASSPI thin films observed during hydration.

Conclusion

As described herein, the influence of the semi-aliphatic backbone for the molecular ordering and proton conductivity was discussed for the sulfonated polyimide thin films. A new alkyl sulfonated polyimide that was less planarity for the main chain was synthesized. The lower molecular weight of sulfonated polyimide was a non-oriented lamellar structure at 70–95% RH condition. However, the higher molecular weight enhanced the degree of molecular ordering and gave the oriented lamellar organized structure by the lyotropic LC property. The reason for the structural difference might derive from the amount of shorter main chains in ASSPI.

Moreover, proton conductivity was enhanced in the case of lamellar organized structure in the same water amount and dissociation state of protons. We concluded that higher proton conductivity was achieved with the oriented lamellar organized structure.

Acknowledgement

This work was supported in part by the Nanotechnology Platform Program (Molecule and Material Synthesis) of the Ministry of Education, Culture, Sports, Science and Technology (MEXT), Japan. This work was partially supported by Iketani Science and Technology Foundation (ISTF), JAPAN.

References

1. Nagao, Y. Proton-Conductivity Enhancement in Polymer Thin Films. Langmuir 33, 12547-12558 (2017).

2. Shannon, M.A., Bohn, P.W., Elimelech, M., Georgiadis, J.G., Mariñas, B.J., & Mayes, A.M. Science and technology for water purification in the coming decades. Nature 452, 301 (2008).

3. Peckham, T.J., & Holdcroft, S. Structure-Morphology-Property Relationships of Non-Perfluorinated Proton-Conducting Membranes. Adv. Mater. 22, 4667-4690 (2010).

4. Nagao, Y., Matsui, J., Abe, T., Hiramatsu, H., Yamamoto, H., Miyashita, T., Sata, N., & Yugami, H. Enhancement of Proton Transport in an Oriented Polypeptide Thin Film. Langmuir 29, 6798-6804 (2013).

5. Amiri, H., Shepard, K.L., Nuckolls, C., & Hernández Sánchez, R. Single-Walled Carbon Nanotubes: Mimics of Biological Ion Channels. Nano Lett. 17, 1204-1211 (2017).

6. Kato, T., Mizoshita, N., & Kishimoto, K. Functional liquid-crystalline assemblies: Self-organized soft materials. Angew. Chem. Int. Ed. 45, 38-68 (2006).

7. Kato, T., Yoshio, M., Ichikawa, T., Soberats, B., Ohno, H., & Funahashi, M. Transport of ions and electrons in nanostructured liquid crystals. Nat. Rev. Mater. 2, 17001 (2017).

8. Soberats, B., Yoshio, M., Ichikawa, T., Zeng, X., Ohno, H., Ungar, G., & Kato, T. Ionic Switch Induced by a Rectangular–Hexagonal Phase Transition in Benzenammonium Columnar Liquid Crystals. J. Am. Chem. Soc. 137, 13212-13215 (2015).

9. Chen, Y., Lingwood, M.D., Goswami, M., Kidd, B.E., Hernandez, J.J., Rosenthal, M., Ivanov, D.A., Perlich, J., Zhang, H., Zhu, X., Möller, M., & Madsen, L.A. Humidity-Modulated Phase Control and Nanoscopic Transport in Supramolecular Assemblies. J. Phys. Chem. B 118, 3207-3217 (2014).

10. Hernandez, J.J., Zhang, H., Chen, Y., Rosenthal, M., Lingwood, M.D., Goswami, M., Zhu, X., Moeller, M., Madsen, L.A., & Ivanov, D.A. Bottom-Up Fabrication of Nanostructured Bicontinuous and Hexagonal Ion-Conducting Polymer Membranes. Macromolecules 50, 5392-5401 (2017).

11. Tonozuka, I., Yoshida, M., Kaneko, K., Takeoka, Y., & Rikukawa, M. Considerations of polymerization method and molecular weight for proton-conducting poly(p-phenylene) derivatives. Polymer 52, 6020-6028 (2011).

12. Lee, J.H., Han, K.S., Lee, J.S., Lee, A.S., Park, S.K., Hong, S.Y., Lee, J.-C., Mueller, K.T., Hong, S.M., & Koo, C.M. Facilitated Ion Transport in Smectic Ordered Ionic Liquid Crystals. Adv. Mater. 28, 9301-9307 (2016).

13. Mauritz, K.A., & Moore, R.B. State of understanding of Nafion. Chem. Rev. 104, 4535-4585 (2004).

14. Li, N., & Guiver, M.D. Ion Transport by Nanochannels in Ion-Containing Aromatic Copolymers. Macromolecules 47, 2175-2198 (2014).

15. He, G., Li, Z., Zhao, J., Wang, S., Wu, H., Guiver, M.D., & Jiang, Z. Nanostructured Ion-Exchange Membranes for Fuel Cells: Recent Advances and Perspectives. Advanced Materials 27, 5280-5295 (2015).

16. Kreuer, K.D. On the development of proton conducting polymer membranes for hydrogen and methanol fuel cells. J. Membr. Sci. 185, 29-39 (2001).

17. Hickner, M.A., Ghassemi, H., Kim, Y.S., Einsla, B.R., & McGrath, J.E. Alternative polymer systems for proton exchange membranes (PEMs). Chem. Rev. 104, 4587-4611 (2004).

18. Kusoglu, A., & Weber, A.Z. New Insights into Perfluorinated Sulfonic-Acid Ionomers. Chem. Rev. 117, 987-1104 (2017).

19. Karan, K. PEFC catalyst layer: Recent advances in materials, microstructural characterization, and modeling. Curr. Opin. Electrochem. 5, 27-35 (2017).

20. Krishnan, K., Yamada, T., Iwatsuki, H., Hara, M., Nagano, S., Otsubo, K., Sakata, O., Fujiwara, A., Kitagawa, H., & Nagao, Y. Influence of Confined Polymer Structure on Proton Transport Property in Sulfonated Polyimide Thin Films. Electrochemistry 82, 865-869 (2014).

21. Krishnan, K., Iwatsuki, H., Hara, M., Nagano, S., & Nagao, Y. Proton conductivity enhancement in oriented, sulfonated polyimide thin films. J. Mater. Chem. A 2, 6895-6903 (2014).

22. Krishnan, K., Iwatsuki, H., Hara, M., Nagano, S., & Nagao, Y. Influence of Molecular Weight on Molecular Ordering and Proton Transport in Organized Sulfonated Polyimide Thin Films. J. Phys. Chem. C 119, 21767-21774 (2015).

23. Nagao, Y., Krishnan, K., Goto, R., Hara, M., & Nagano, S. Effect of Casting Solvent on Interfacial Molecular Structure and Proton Transport Characteristics of Sulfonated Polyimide Thin Films. Anal. Sci. 33, 35-39 (2017).

24. Wakita, J., Jin, S., Shin, T.J., Ree, M., & Ando, S. Analysis of Molecular Aggregation Structures of Fully Aromatic and Semialiphatic Polyimide Films with Synchrotron Grazing Incidence Wide-Angle X-ray Scattering. Macromolecules 43, 1930-1941 (2010).

25. Ono, Y., Goto, R., Hara, M., Nagano, S., Abe, T., & Nagao, Y. High Proton Conduction of Organized Sulfonated Polyimide Thin Films with Planar and Bent Backbones. Macromolecules 51, 3351-3359 (2018).

26. Sirringhaus, H., Brown, P.J., Friend, R.H., Nielsen, M.M., Bechgaard, K., Langeveld-Voss, B.M.W., Spiering, A.J.H., Janssen, R.A.J., Meijer, E.W., Herwig, P., & de Leeuw, D.M. Two-dimensional charge transport in self-organized, high-mobility conjugated polymers. Nature 401, 685 (1999).

27. Nagano, S., Kodama, S., & Seki, T. Ideal Spread Monolayer and Multilayer Formation of Fully Hydrophobic Polythiophenes via Liquid Crystal Hybridization on Water. Langmuir 24, 10498-10504 (2008).

28. Nagano, S. Inducing Planar Orientation in Side‐Chain Liquid‐Crystalline Polymer Systems via Interfacial Control. Chem. Rec. 16, 378-392 (2016).

29. Sato, T., Hayasaka, Y., Mitsuishi, M., Miyashita, T., Nagano, S., & Matsui, J. High Proton Conductivity in the Molecular Interlayer of a Polymer Nanosheet Multilayer Film. Langmuir 31, 5174-5180 (2015).

30. Sato, T., Tsukamoto, M., Yamamoto, S., Mitsuishi, M., Miyashita, T., Nagano, S., & Matsui, J. Acid-Group-Content-Dependent Proton Conductivity Mechanisms at the Interlayer of Poly(N-dodecylacrylamide-co-acrylic acid) Copolymer Multilayer Nanosheet Films. Langmuir 33, 12897-12902 (2017).

31. Matsui, J., Miyata, H., Hanaoka, Y., & Miyashita, T. Layered Ultrathin Proton Conductive Film Based on Polymer Nanosheet Assembly. ACS Appl. Mater. Inter. 3, 1394-1397 (2011).

32. Saito, J., Miyatake, K., & Watanabe, M. Synthesis and properties of polyimide ionomers containing 1H-1,2,4-triazole groups. Macromolecules 41, 2415-2420 (2008).

33. Miyahara, T., Miyake, J., Matsuno, S., Watanabe, M., & Miyatake, K. A sulfonated polybenzophenone/polyimide copolymer as a novel proton exchange membrane. RSC Adv. 5, 50082-50086 (2015).

34. Chang, Y., Brunello, G.F., Fuller, J., Hawley, M., Kim, Y.S., Disabb-Miller, M., Hickner, M.A., Jang, S.S., & Bae, C. Aromatic Ionomers with Highly Acidic Sulfonate Groups: Acidity, Hydration, and Proton Conductivity. Macromolecules 44, 8458-8469 (2011).

35. Kunimatsu, K., Yagi, K., Bae, B., Miyatake, K., Uchida, H., & Watanabe, M. ATR-FTIR Analysis of the State of Water in a Sulfonated Block Poly(arylene ether sulfone ketone) Membrane and Proton Conductivity Measurement during the Hydration/Dehydration Cycle. J. Phys. Chem. C 117, 3762-3771 (2013).

Graphical Abstract

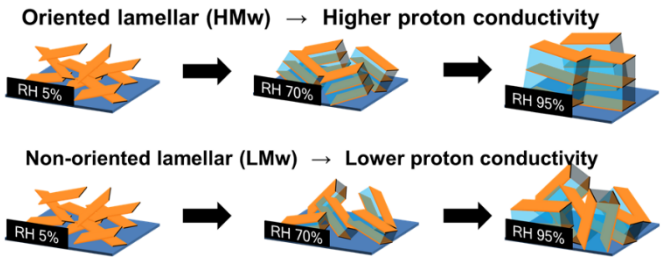

High-molecular-weight (HM_w) sulfonated polyimide thin films with the semi-aliphatic main chain exhibited the oriented lamellar structure and high proton conductivity (1.5×10^{-1} S cm^{-1}) under a humidified condition. Low-molecular-weight (LM_w) sulfonated polyimide thin films with the same semi-aliphatic backbone exhibited the non-oriented lamellar structure and low proton conductivity (3.0×10^{-2} S cm^{-1}) under a humidified condition. Results indicate that, in sulfonated polyimide thin films with semi-aliphatic main chain, the lamellar orientation greatly contributes to the high proton conductivity.